Electronic Supplementary Information for Dalton Transactions

Mononuclear Fe(II)-N4Py complexes in oxidative DNA cleavage: structure, activity and mechanism

Qian Li, Tieme A. van den Berg, Ben L. Feringa* and Gerard Roelfes*

Stratingh Institute form Chemsitry, University of Groningen,
Nijenborgh 4, 9747AG , Groningen, The Netherlands

Supplementary Information

Syntheses

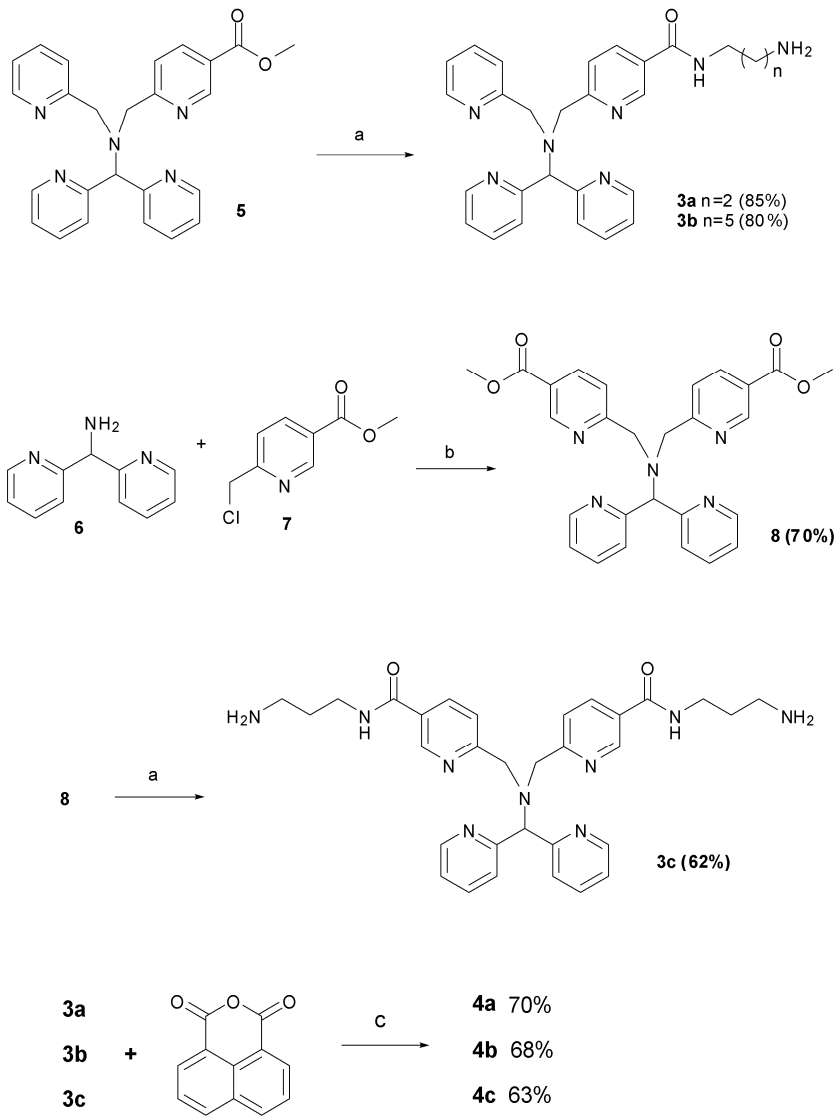

Scheme S1: Synthesis of ligands **1-4**. (a) Corresponding diamine, NaCN, MeOH, reflux overnight; (b) iPr$_2$EtN, CH_3CN, reflux overnight; (c) MeOH, reflux overnight.

Dimethyl 6,6'-(dipyridin-2-ylmethylazanediyl)bis(methylene) dinicotinate (8)

A solution of **6**[1](430 mg, 2.3 mmol), **7** (1.27 g, 6.8 mmol) and *i*Pr_2EtN (9.2 mmol, 1.6 mL) in MeCN (15 mL) was heated under reflux overnight under a N_2 atmosphere. After cooling down to room temperature, the solvent was evaporated and the residue was purified by column chromatography (Al_2O_3 neutral act. I, EtOAc/heptane/Et_3N 10:5:1) to yield **8** (716 mg, 70%) as a viscous brown liquid. ^{1}H NMR (300 MHz, $CDCl_3$): δ = 9.08 (d, J = 2.1 Hz, 2 H), 8.57 (d, J = 4.8 Hz, 2H), 8.20 (dd, J = 8.1 Hz, 2.1 Hz, 2H), 7.72-7.60 (m, 6H), 7.15 (m, 2H), 5.34 (s, 1H), 4.07 (s, 4H), 3.93 (s, 6H); ^{13}C NMR (75 MHz, $CDCl_3$): δ = 165.7, 164.4, 159.5, 150.1, 149.2, 137.2, 136.2, 124.1, 123.8, 122.4, 122.1, 72.4, 72.3, 57.4, 52.2, 52.1; MS (ESI^+): *m/z*: 484.4, $[M + H]^+$.

Table S1: ESI-MS data for Fe(II) complexes of ligands 4a-c generated *in situ*.

ligand	MS (ESI^+): *m/z*		
4a	748.4 $[M\text{-}Fe^{2+}\text{-}HCOO^-]^+$	372.4 $[M\text{-}Fe^{2+}\text{-}(MeCN)]^{2+}$	351.8 $[M\text{-}Fe^{2+}]^{2+}$
4b	790.4 $[M\text{-}Fe^{2+}\text{-}HCOO^-]^+$	372.8 $[M\text{-}Fe^{2+}]^{2+}$	
4c	1079.0 $[M\text{-}Fe^{2+}\text{-}H^+\text{-}SO_4^{2-}]^+$	1028.5 $[M\text{-}Fe^{2+}\text{-}HCOO^-]^+$	512.5 $[M\text{-}Fe^{2+}\text{-}(MeCN)]^{2+}$

DNA cleavage in the presence of DTT

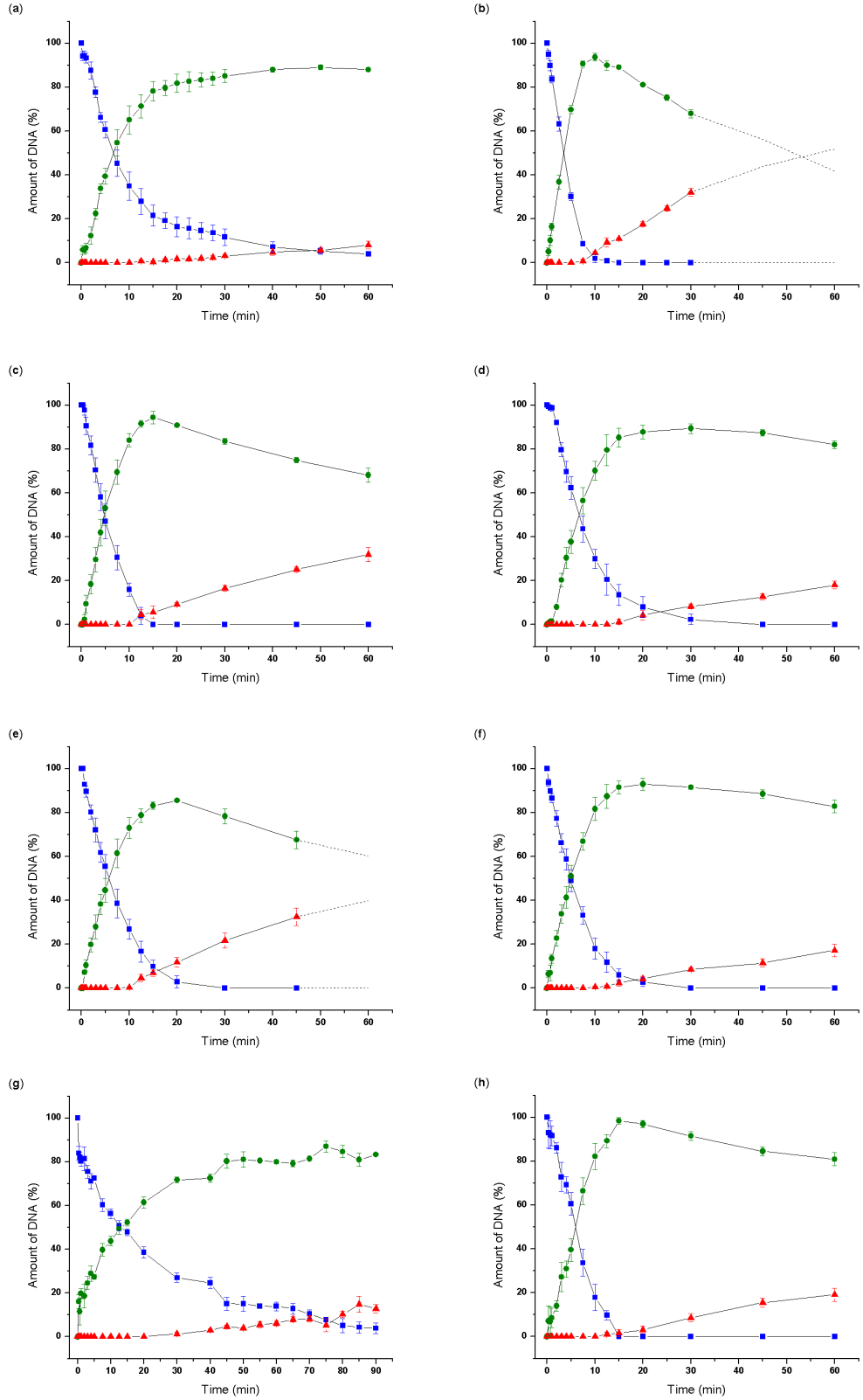

Figure S1: Time profile for cleavage of supercoiled DNA (■) to nicked (●) and linear (▲) DNA in 10 mM Tris.Cl (pH 8.0) at 37 ºC with 1 mM DTT and (a) Fe(II)-**1**; (b) Fe(II)-**2**; (c) Fe(II)-**3a**; (d) Fe(II)-**3b**; (e) Fe(II)-**3c**; (f) Fe(II)-**4a**; (g) Fe(II)-**4b** (more data points were taken to get a good *m*/*n* plot); (h) Fe(II)-**4c**. Conditions: 1.0 μM complex, 0.1 μg μL^{-1} pUC18 plasmid DNA (150 μM bp).

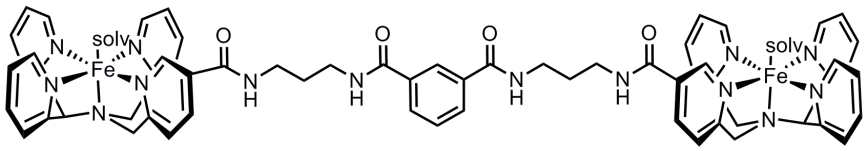

Figure S2: Structure of di-nuclear Fe(II)N4Py complex Fe(II)-**L**.

Rate of DNA cleavage: To determine the order of DNA cleavage reaction, different concentrations of DTT were employed in DNA cleavage with Fe(II)-**1**. Without DTT as reducing agent, 14% of the substrate supercoiled DNA was cleaved after 30 min, corresponding to 0.15 (+/- 0.03) single strand cuts per DNA molecule, calculated with Equation S1. When one equiv. of DTT respect to Fe(II)-**1** was added, 60% nicked DNA was formed within 30 min, corresponding to 0.92 (+/- 0.06) single-strand cuts per DNA molecule. Higher concentrations of DTT (from 0.01 mM to 1.0 mM) resulted in a dramatic increase in DNA cleavage, as the number of single-strand cut per DNA molecule increased by a factor of six (Figure S3). It should be noted that when linear DNA is present and Equation S2 is used to calculate the number of single-strand cuts (*n*), relatively large error margins are observed. This is due to the fact that small deviations in the amount of linear DNA results in large differences in the values of *n* calculated from equation S2.

$$f_I = e^{-n}$$

Equation S1: Average number of single-strand cuts (*n*) per DNA molecule, calculated from the fraction of supercoiled DNA (f_I).

$$f_I + f_{II} = \left[1 - n(2h+1)/2L\right]^{n/2}$$

Equation S2: Average number of single-strand cuts (*n*) per DNA molecule, calculated from the fractions of supercoiled DNA (f_I) and nicked DNA (f_{II}), maximum distance between two cuts on opposite strands for generating one double strand cut (*h*), *i.e.* 16 base pairs[2], and the total number of base pairs of the substrate plasmid DNA (*L*), *i.e.* 2686.

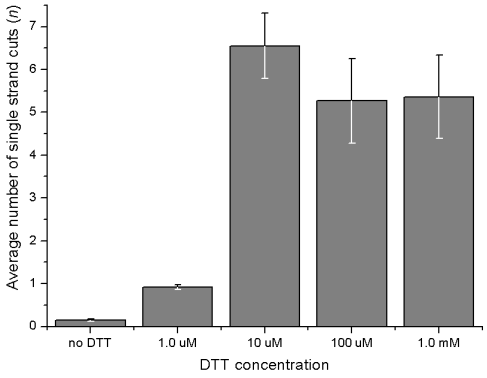

Figure S3: Calculated average number of single-strand cuts per DNA molecule (*n*) with different concentrations of DTT at 30 min. Error bars represent the uncertainty limits of the data, based on a Monte Carlo simulation, taking into account a standard deviation σ of 0.03 of the individual DNA fractions. Conditions: 1.0 μM complex, 0.1 μg μL^{-1} pUC18 plasmid DNA (150 μM bp), 10 mM Tris.Cl (pH 8.0) at 37 ºC.

Since DNA cleavage reactions were performed at a final concentration of 1.0 mM DTT (1000 equiv. corresponding to Fe(II)-**1**), all the DNA cleavage in the presence of DTT in this study were considered as pseudo-first-order reaction, therefore, the decrease in the amount of supercoiled DNA in time can be used to calculate k_{obs} for DNA cleavage. The natural logarithm of f_I was plotted as a function of time, and from the slope of the linear fit the value of k_{obs} was determined (Figure S4).[3] k_{obs} for DNA cleavage induced by Fe(II)-**1** in the presence of DTT was calculated to be ~ 0.1 min^{-1}. In the case of Fe(II)-**2**, the fraction of supercoiled DNA was small because of the faster DNA cleavage process, which led to large uncertainties in the data (the error σ is equal to $\sigma_{[DNA]}$/[DNA], Equation S3) and consequently a reliable estimation of k_{obs} was not obtained.

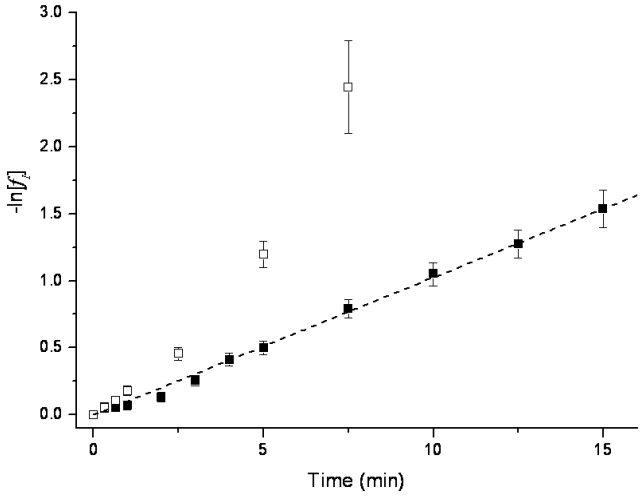

Figure S4: -Ln[f_I] plotted as a function of time for Fe(II)-**1** (■) and Fe(II)-**2** (□). The dashed line is the linear fit of the data of Fe(II)-**1** (k_{obs} = 0.103 +/- 0.002 min^{-1}, R^2 = 0.997). Error bars represent the expected deviation, based on a standard deviation σ of 0.03 in the fraction of supercoiled DNA (f_I).

$$\sigma_f = \left|\frac{df}{dx}\right|\sigma_x$$

Equation S3: Expected error in the function *f* from the error in *x*, where σ_x is the error in *x* and σ_f is the expected error in $f(x)$.[4]

Alternatively, the number of single-strand cuts per DNA molecule (n) can be calculated at different time points by using Equation S1 and S2 for DNA cleavage process with Fe(II)-**1** and Fe(II)-**2**. The calculated values of n can be plotted as a function of time and from the slope of the linear fit the rate constant of single-strand DNA cleavage can be obtained (Figure S5). The rate constant of single-strand DNA cleavage induced by Fe(II)-**1** determined from the slope of the graph is 0.095 +/- 0.003 min^{-1}, corresponding well to the k_{obs} value (0.103 +/- 0.002 min^{-1}, R^2 = 0.997). With Fe(II)-**2**, a four-fold increase in the rate constant is observed (0.379 +/- 0.011 min^{-1}, R^2 = 0.984), indicating a positive influence of the DNA binding unit 9-aminoacridine. The well-fit linear relationship between n and time further indicates that

only single-strand cleavage happened in DNA cleavage process. As more data points can be taken to calculate the rate constant, this approach is much better for very active single strand DNA cleaving agents.

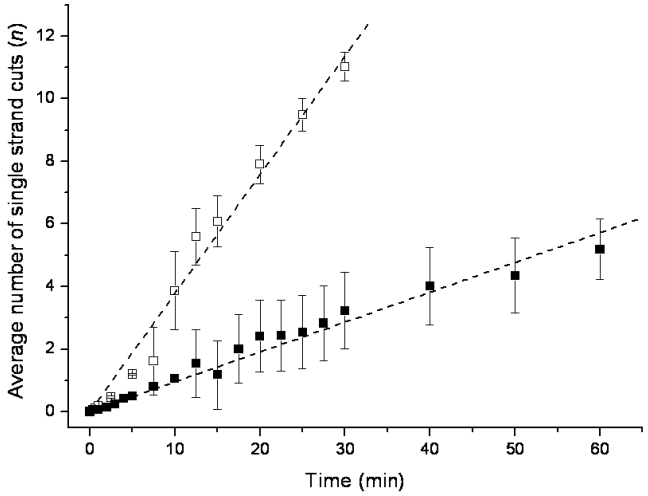

Figure S5: Average number of single strand cuts per DNA molecule (*n*) as a function of time for Fe(II)-**1** (■) and Fe(II)-**2** (□). Dashed lines represent the linear fit through the data points for Fe(II)-**1** (0.095 +/- 0.003 min^{-1}, R^2 = 0.976) and Fe(II)-**2** (0.379 +/- 0.011 min^{-1}, R^2 = 0.984). Error bars represent the uncertainty limits of the data, based on a Monte Carlo simulation, taking into account a standard deviation σ of 0.03 of the individual DNA fractions.

The DNA cleavage efficiency of complexes are dependent on the concentrations of DNA ([DNA]) and complexes ([complex]), however, in the calculations of k_{obs} by using both of the two methods metioned above, [DNA] and [complexes] were not taken into account. Resultingly, the values of k_{obs} do not indicate the DNA cleavage efficiency of complexes properly. Therefore, taking account [DNA] and [complexes], k_{obs} is corrected to k^* by using Equation S4. k^* for Fe(II)-**1** and Fe(II)-**2** are 0.0054 +/- 0.0002 min^{-1} and 0.022 +/- 0.001 min^{-1}, respectively.

$$k^* = k_{obs} \times \frac{[DNA]}{[complex]}$$

Equation S4: Correction of k_{obs} by taking account of concentrations of DNA (0.1 μg μL^{-1}, 56.4 nM) and complexes (1.0 μM).

It is difficult to compare the kinetic results for DNA cleavage by our Fe(II)-N4Py complexes with other single-strand DNA cleaving agents in literature, because often different reaction conditions (*e.g.* pH, temperature, buffer) are used.

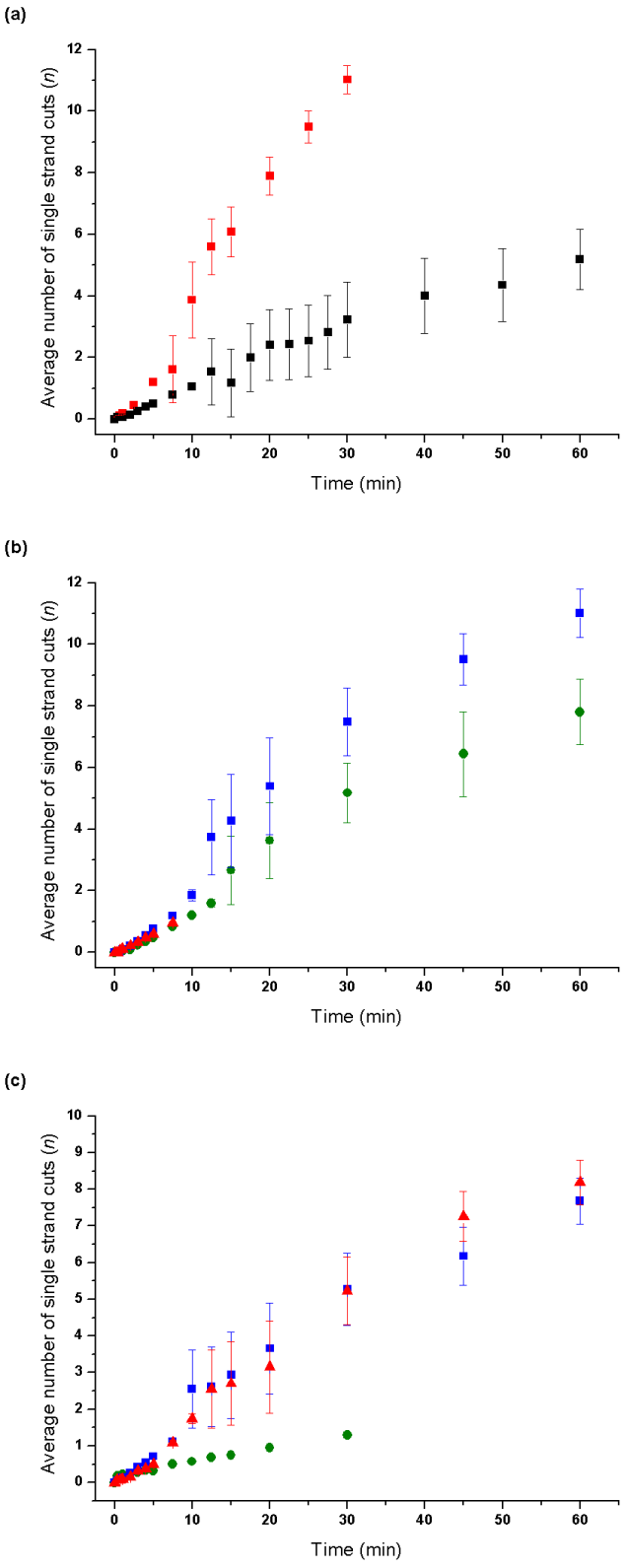

Figure S6: Number of single-strand cuts per DNA molecule (*n*) as a function of for (a) Fe(II)-**1** (■), Fe(II)-**2** (■); (b) Fe(II)-**3a** (■), Fe(II)-**3b** (●), Fe(II)-**3c** (▲); (c) Fe(II)-**4a** (■), Fe(II)-**4b** (●), Fe(II)-**4c** (▲). Conditions: 1.0 μM complex, 0.1 μg μL^{-1} pUC18 plasmid DNA (150 μM bp), 10 mM Tris.Cl (pH 8.0), 1 mM DTT, 37 ºC.

DNA cleavage in the absence of DTT

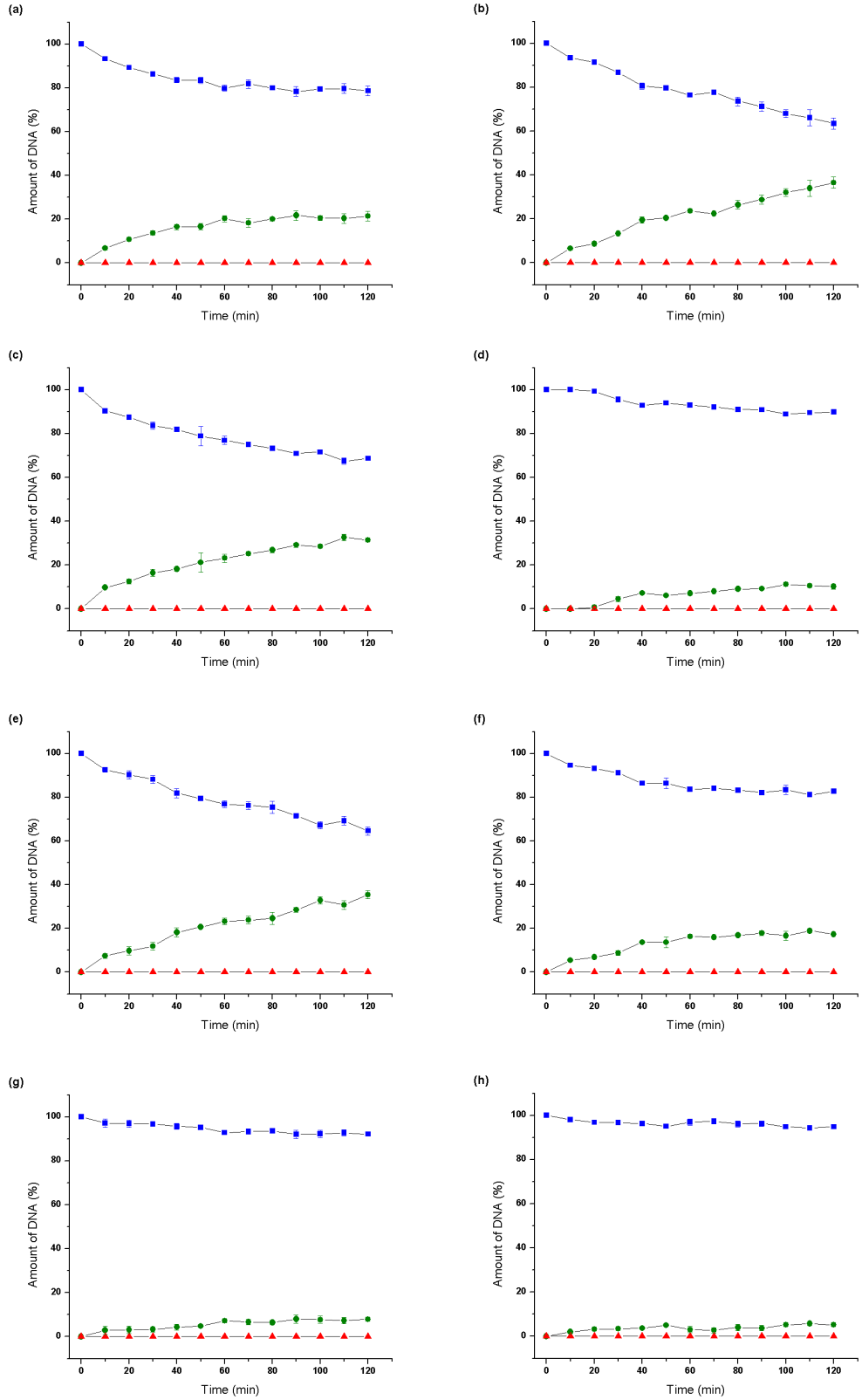

Figure S7: Time profile for cleavage of supercoiled DNA (■) to nicked (●) and linear (▲) DNA in 10 mM Tris.Cl (pH 8.0) at 37 ºC with (a) Fe(II)-**1**; (b) Fe(II)-**2**; (c) Fe(II)-**3a**; (d) Fe(II)-**3b**; (e) Fe(II)-**3c**; (f) Fe(II)-**4a**; (g) Fe(II)-**4b**; (h) Fe(II)-**4c**. Conditions: 1.0 μM complex, 0.1 μg μL^{-1} pUC18 plasmid DNA (150 μM bp).

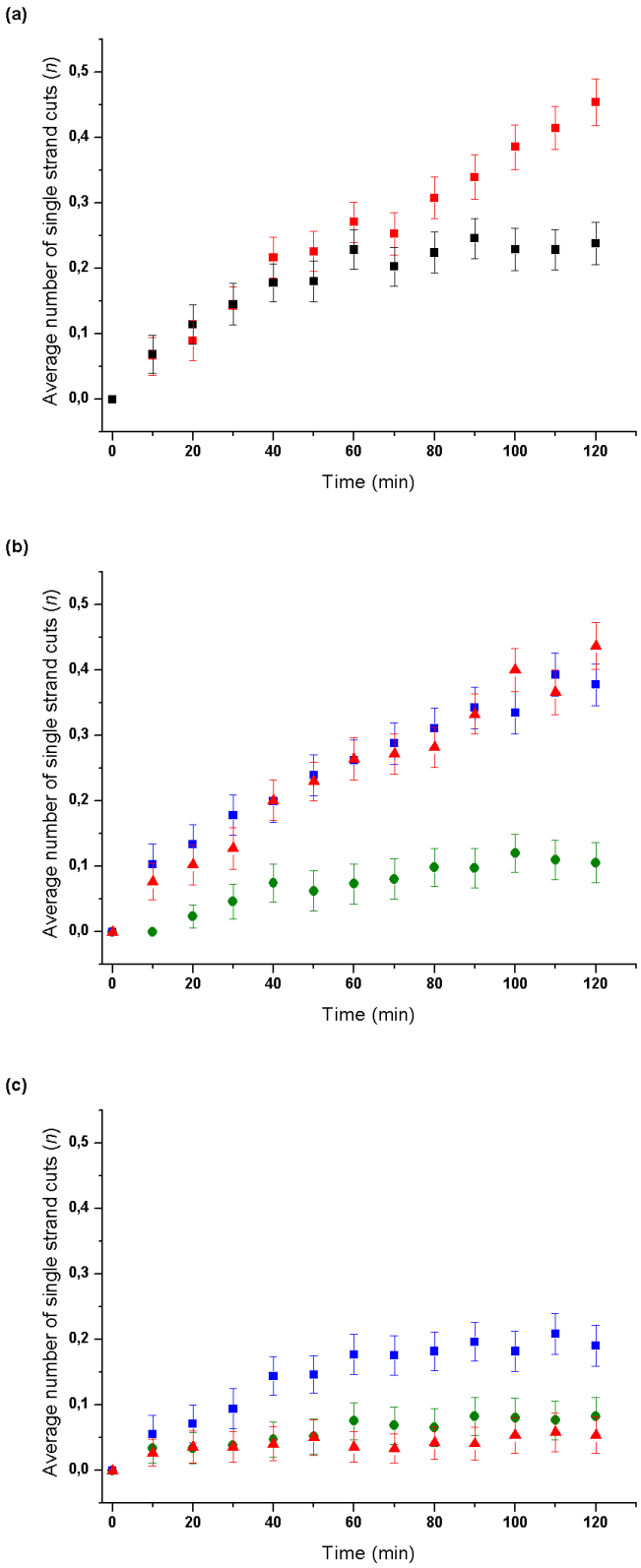

Figure S8: Number of single-strand cuts per DNA molecule (*n*) as a function of time for (a) Fe(II)-**1** (■), Fe(II)-**2** (■); (b) Fe(II)-**3a** (■), Fe(II)-**3b** (●), Fe(II)-**3c** (▲); (c) Fe(II)-**4a** (■), Fe(II)-**4b** (●), Fe(II)-**4c** (▲). Conditions: 1.0 μM complex, 0.1 μg μL^{-1} pUC18 plasmid DNA (150 μM bp), 10 mM Tris.Cl (pH 8.0), 37 ºC.

Table S2: k_{obs} of DNA cleavage in the presence and absence of reductant.

No.	complex	k_{obs} (min^{-1})	
		DTT	No DTT
1	Fe^{II}-**1**	0.095 ± 0.003, R^2 = 0.976	0.0035 ± 0.0003, R^2 = 0.947[b]
2	Fe^{II}-**2**	0.379 ± 0.011, R^2 = 0.984	0.0035 ± 0.0001, R^2 = 0.979
3	Fe^{II}-**3a**	0.209 ± 0.009, R^2 = 0.958	0.0029 ± 0.0003, R^2 = 0.943
4	Fe^{II}-**3b**	0.142 ± 0.005, R^2 = 0.973	[c]
5	Fe^{II}-**3c**	0.122 ± 0.003, R^2 = 0.993[a]	0.0033 ± 0.0003, R^2 = 0.969
6	Fe^{II}-**4a**	0.145 ± 0.004, R^2 = 0.944	0.0028 ± 0.0002, R^2 = 0.965[b]
7	Fe^{II}-**4b**	0.040 ± 0.001, R^2 = 0.995[a]	[c]
8	Fe^{II}-**4c**	0.152 ± 0.005, R^2 = 0.978	[c]

1 μM iron complex, 0.1 μg μL^{-1} supercoiled pUC18 DNA (150 μM bp), 10 mM Tris.Cl buffer (pH 8.0), 37 ºC, with or without 1 mM DTT. [a] In the presence of DTT, for double-strand cleaving agents Fe(II)-**3c** and Fe(II)-**4b**, only single-strand cuts occurred before linear DNA was formed and rate constants for the single-strand cleavage process can be determined. With Fe(II)-**3c** and Fe(II)-**4b**, linear DNA appeared after 7.5 min and 30 min respectively (Figure S1 and S6); [b] In the absence of DTT, with Fe(II)-**1** and Fe(II)-**4a**, the formation of nicked DNA stopped increasing after 60 min so the rate constants are calculated for single-strand cleavage within 60 min (Figure S7 and S8); [c] The cleavage rate can not be obtained through the small numbers of single-strand cuts (Figure S8).

DNA cleavage with Fe(II)-BLM

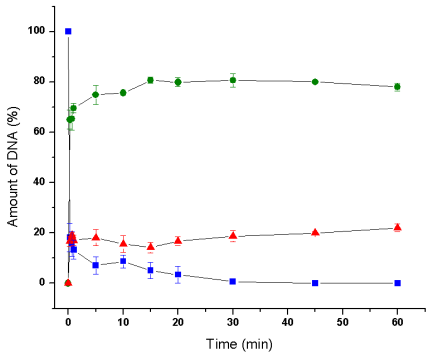

Figure S9: Time profile for cleavage supercoiled DNA (■) to nicked (●) and linear (▲) DNA with Fe(II)-BLM in Tris.Cl (pH 8.0) at 37 ºC. Conditions: 1.0 μM complex (with respect to Fe^{II}), 0.1 μg μL^{-1} pUC18 plasmid DNA (150 μM bp), 1mM DTT.

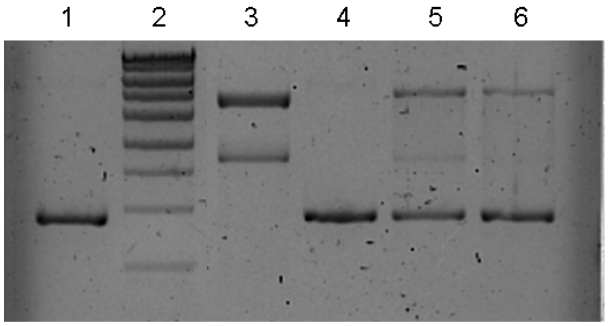

Figure S10: Agarose gel picture of DNA Cleavage with 0.1 μg μL^{-1} supercoiled pUC18 DNA (150 μM bp), Tris.Cl buffer (pH 8.0), 37 ºC. Lane 1, DNA reference; lane 2, DNA ladder; lane 3, 1 μM Fe(II)-BLM, 1 mM DTT, 60 min; lane 4, 1 μM BLM, 60 min; lane 5, 1 μM Fe(II)-BLM, 1 min; lane 6, 1 μM Fe(II)-BLM, 60 min.

DNA cleavage with iron salts

DNA cleavage with iron salts in the presence of reductant: DNA Cleavage activities of the iron salts, $(NH_4)_2Fe^{II}(SO_4)_2.6H_2O$ and $NH_4Fe^{III}(SO_4)_2.12H_2O$, were determined with DTT within 60 min. The time dependence of the DNA cleavage with these two iron salts is shown in Figure S11, and Table S2. Less amounts of DNA cleavage (46% and 12%, respectively) were observed with Fe(II) and Fe(III) salts within 10 min, compared to the efficient DNA cleavage (> 60% within 10 min) with all of Fe(II)N4Py complexes except Fe(II)-**4b** in the present study.

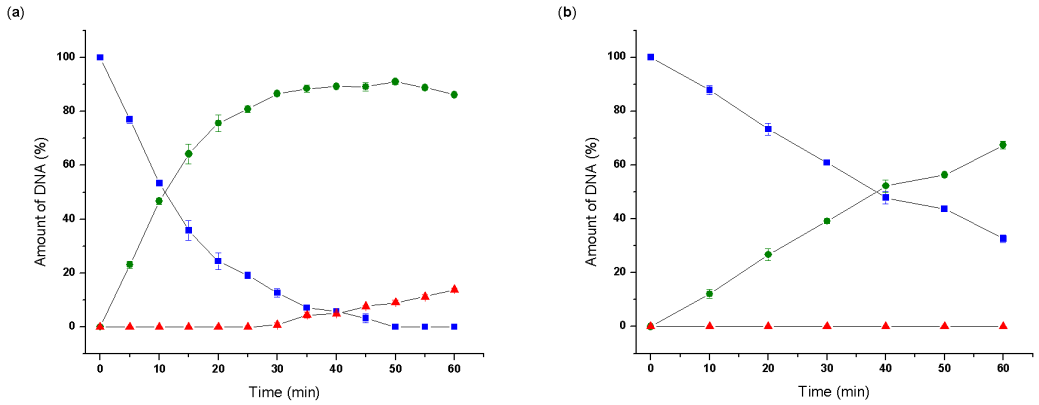

Figure S11: Time profile for cleavage of supercoiled DNA (■) to nicked (●) and linear (▲) DNA in 10 mM Tris.Cl (pH 8.0) at 37 ºC with (a) $(NH_4)_2Fe^{II}(SO_4)_2.6H_2O$ and (b) $NH_4Fe^{III}(SO_4)_2.12H_2O$. Conditions: 1.0 μM complex (with respect to Fe(II), 0.1 μg μL^{-1} pUC18 plasmid DNA (150 μM bp) with 1 mM DTT.

Table S3: DNA cleavage in the presence of reductant.

reagents	Time (min)	Supercoiled DNA (%)	Nicked DNA (%)	Linear DNA (%)	dsc *vs.* ssc
$(NH_4)_2Fe^{II}(SO_4)_2.6H_2O$	10	54 +/- 1	46 +/- 1	0	ssc
	60	1 +/- 1	90 +/- 1	10 +/- 1	
$NH_4Fe^{III}(SO_4)_2.12H_2O$	10	88 +/- 2	12 +/- 2	0	ssc
	60	33 +/- 2	67 +/- 2	0	

1 µM iron salt, 0.1 µg µL^{-1} supercoiled pUC18 DNA (150 µM bp), 1 mM DTT, Tris.Cl buffer (pH 8.0), 37 ºC. A correction factor of 1.31 is used for the reduced EtBr uptake capacity of supercoiled plasmid pUC18 DNA.

Figure S12 is the *m*/*n* plot of the DNA cleavage with $(NH_4)_2Fe^{II}(SO_4)_2.6H_2O$ and $NH_4Fe^{III}(SO_4)_2.12H_2O$ within 60 min. These two iron salts are single-strand DNA cleaving agents. DNA cleavage effected by Fe(III) salts is much slower than the one effected by Fe(II) salts, with a cleavage rate k^* 1.13 (+/- 0.06) × 10^{-3} min^{-1} compared to 4.09 (+/- 0.06) × 10^{-3} min^{-1}. (Figure S13)

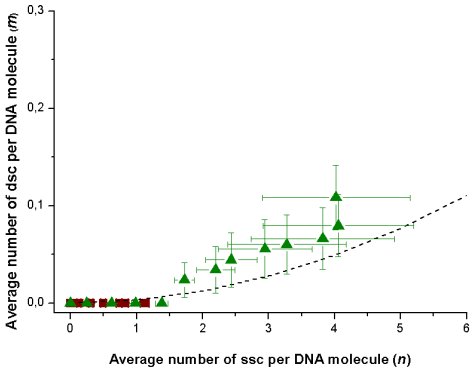

Figure S12: Number of double strand cuts (*m*) as a function of single strand cuts (*n*) per DNA molecule for $(NH_4)_2Fe^{II}(SO_4)_2.6H_2O$ (▲) and $NH_4Fe^{III}(SO_4)_2.12H_2O$ (■).

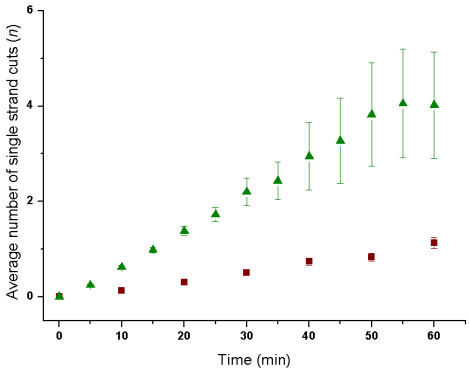

Figure S13: Average number of single strand cuts per DNA molecule (*n*) as a function of time for $(NH_4)_2Fe^{II}(SO_4)_2.6H_2O$ (▲) and $NH_4Fe^{III}(SO_4)_2.12H_2O$ (■). K_{obs} for $(NH_4)_2Fe^{II}(SO_4)_2.6H_2O$ (▲) is 0.073 ± 0.001 min^{-1} (R^2 = 0.995), for $NH_4Fe^{III}(SO_4)_2.12H_2O$ (■) is 0.020 ± 0.001 min^{-1} (R^2 = 0.973). Conditions: 1.0 µM complex, 0.1 µg µL^{-1} pUC18 plasmid DNA (150 µM in bp), 10 mM Tris.Cl (pH 8.0), 1 mM DTT, 37 ºC.

DNA cleavage with iron salts in the absence of reductant: With $(NH_4)_2Fe^{II}(SO_4)_2.6H_2O$ and $NH_4Fe^{III}(SO_4)_2.12H_2O$, no DNA cleavage was achieved within 2 hours in the absence of reducing agent DTT.

Mechanistic probes

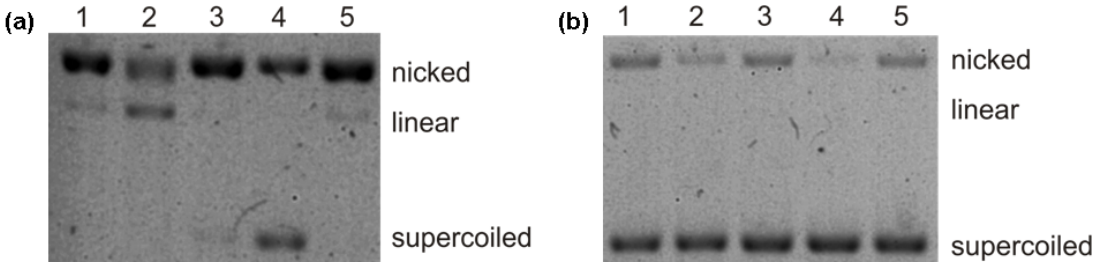

Figure S14: Agarose gel picture of DNA Cleavage with 1 μM Fe(II)-**1**, 0.1 μg μL^{-1} supercoiled pUC18 DNA (150 μM bp), Tris.Cl buffer (pH 8.0), 37 ºC, 30 min, (a) with 1 mM DTT and (b) without 1mM DTT. Lane 1, no ROS scavenger; lane 2, SOD (1.0-5.0 U); lane 3, catalase (1.0-2.5 U); lane 4, SOD(1.0-5.0 U) and catalase (1.0-2.5 U); lane 5, BSA (1 μg).

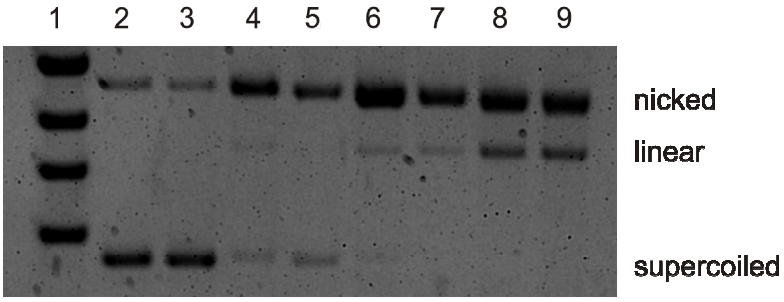

Figure S15: Agarose gel of DNA Cleavage with 1 μM Fe(II)-**1**, 0.1 μg μL^{-1} supercoiled pUC18 DNA (150 μM bp), Tris.Cl buffer (pH 8.0), 37 ºC, 30 min. Lane 1, DNA ladder; lane 2, Fe(II)-**1** (1.0 μM); lane 3, Fe(II)-**1** (1.0 μM) and DMSO (1.0 mM); lane 4, Fe(II)-**1** (1.0 μM) and DTT (1.0 mM); lane 5, Fe(II)-**1** (1.0 μM), DTT (1.0 mM), and DMSO (1.0 mM); lane 6, Fe(II)-**1** (1.0 μM) and H_2O_2 (1.0 mM); lane 7, Fe(II)-**1** (1.0 μM), H_2O_2 (1.0 mM), and DMSO (1.0 mM); lane 8, Fe(II)-**1** (1.0 μM), DTT (1.0 mM), and H_2O_2 (1.0 mM); lane 9, Fe(II)-**1** (1.0 μM), DTT (1.0 mM), H_2O_2 (1.0 mM), and DMSO (1.0 mM).

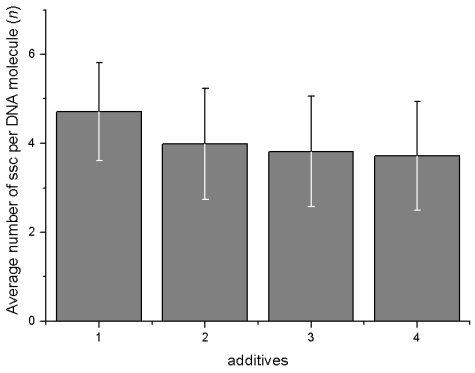

Figure S16: Calculated average number of single strand cuts per DNA molecule (*n*) at 30 min. Column 1, DTT (1.0 mM); Column 2, DTT (1.0 mM) + BSA (1 μg); Column 3, H_2O_2 (1 mM); Column 4, H_2O_2 (1 mM) + BSA (1 μg). Error bars represent the uncertainty limits of the data, based on a Monte Carlo simulation, taking into account a standard deviation σ of 0.03 of the individual DNA fractions. Conditions:1 μM Fe(II)-**1**, 0.1 μg μL^{-1} supercoiled pUC18 DNA (150 μM bp), Tris.Cl buffer (pH 8.0), 37 ºC, 30 min.

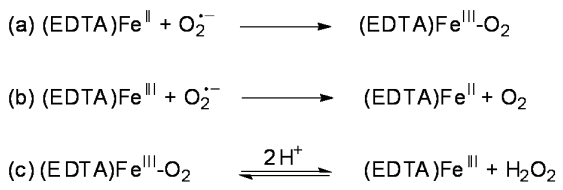

Scheme S2: Reaction of Fe(EDTA) complexes with superoxide radicals.[5,6]

References

[1] (a) M. Lubben, A. Meetsma, E. C. Wilkinson, B. Feringa and L. Que, Jr., *Angew. Chem.*, *Int. Ed. Engl.*, 1995, **34**, 1512; (b) G. Roelfes, M. E. Branum, L. Wang, L. Que, Jr. and B. L. Feringa, *J. Am. Chem. Soc.*, 2000, **122**, 11517.

[2] (a) D. Freifelder and B. Trumbo, *Biopolymers*, 1969, **7**, 681; (b) R. Cowan, C. M. Collis and G. W. Grigg, *J. Theor. Biol.*, 1987, **127**, 229.

[3] P. Atkins, J. De Paula, *Atkins' Physical Chemistry*, 8 ed. W.H. Freeman and Company, New York, 2006.

[4] H. J. C. Berendsen, *Goed Meten met Fouten*, Laboratorium voor Biofysische Chemie, University of Groningen, Groningen, 1997.

[5] G. J. McClune, J. A. Fee, G. A. McCluskey and J. T. Groves, *J. Am. Chem. Soc.*, 1977, **99**, 5220.

[6] C. Bull, G. J. McClune and J. A. Fee, *J. Am. Chem. Soc.*, 1983, **105**, 5290.

^{1}H NMR spectrum of **8** ($CDCl_3$, 25 ºC)

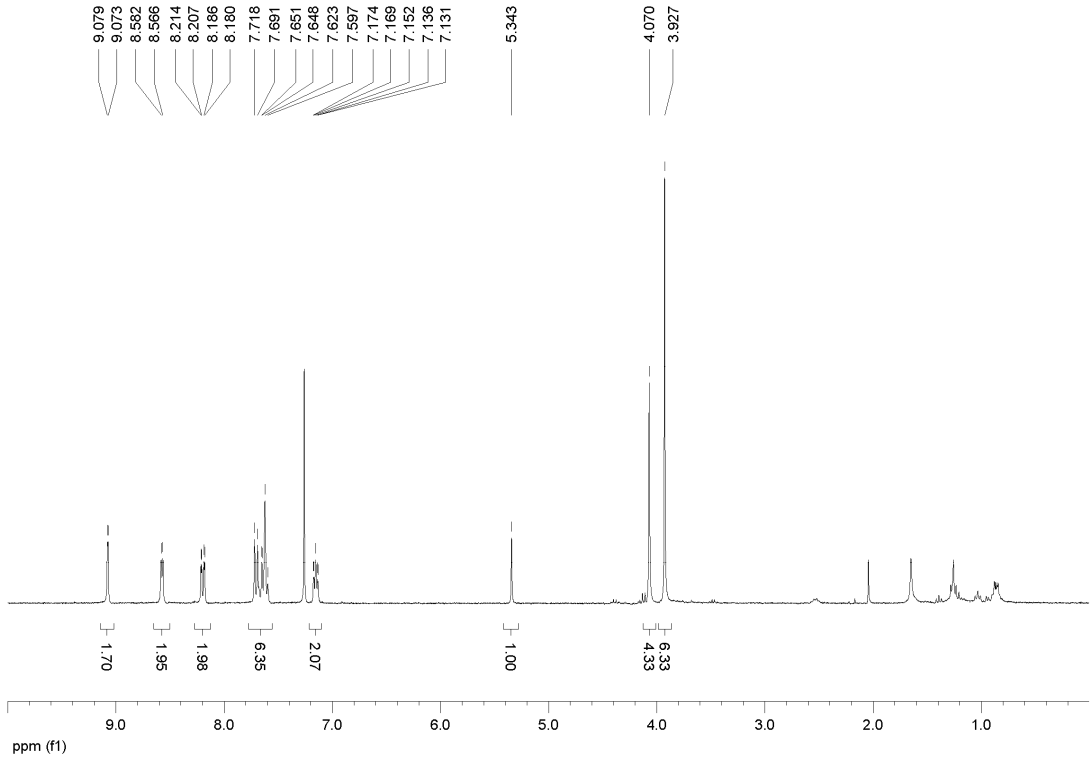

^{13}C NMR spectrum of **8** ($CDCl_3$, 25 ºC)

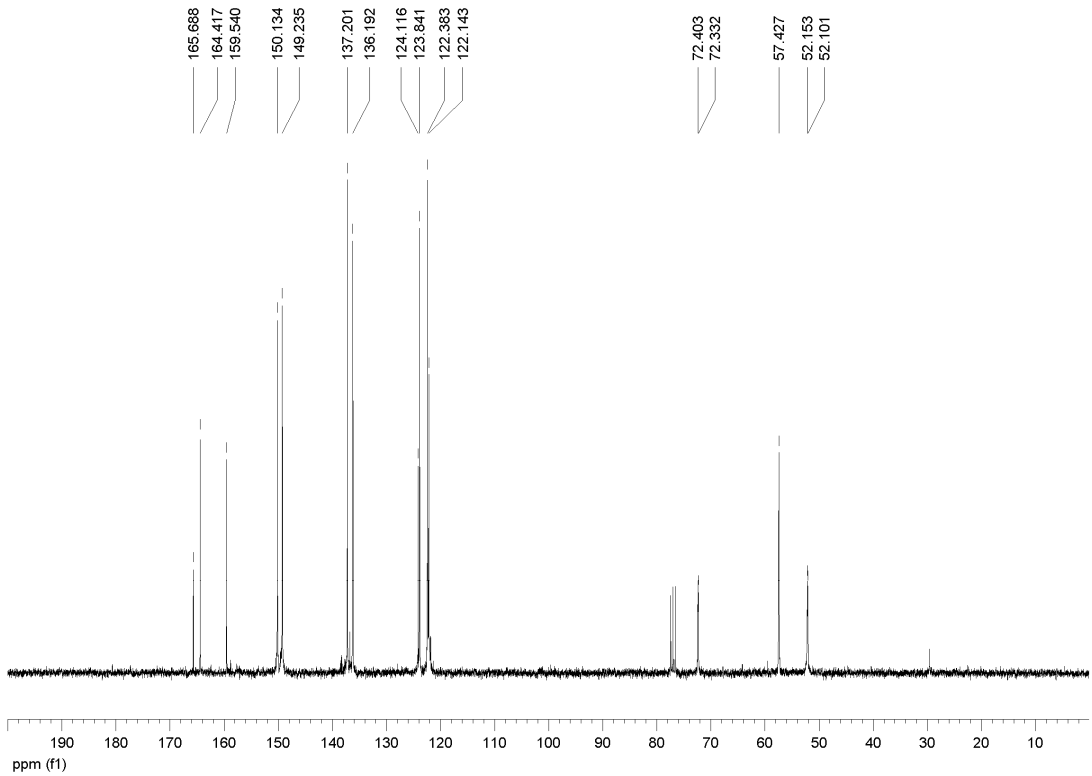

^{1}H NMR spectrum of **3b** ($CDCl_3$, 25 ºC)

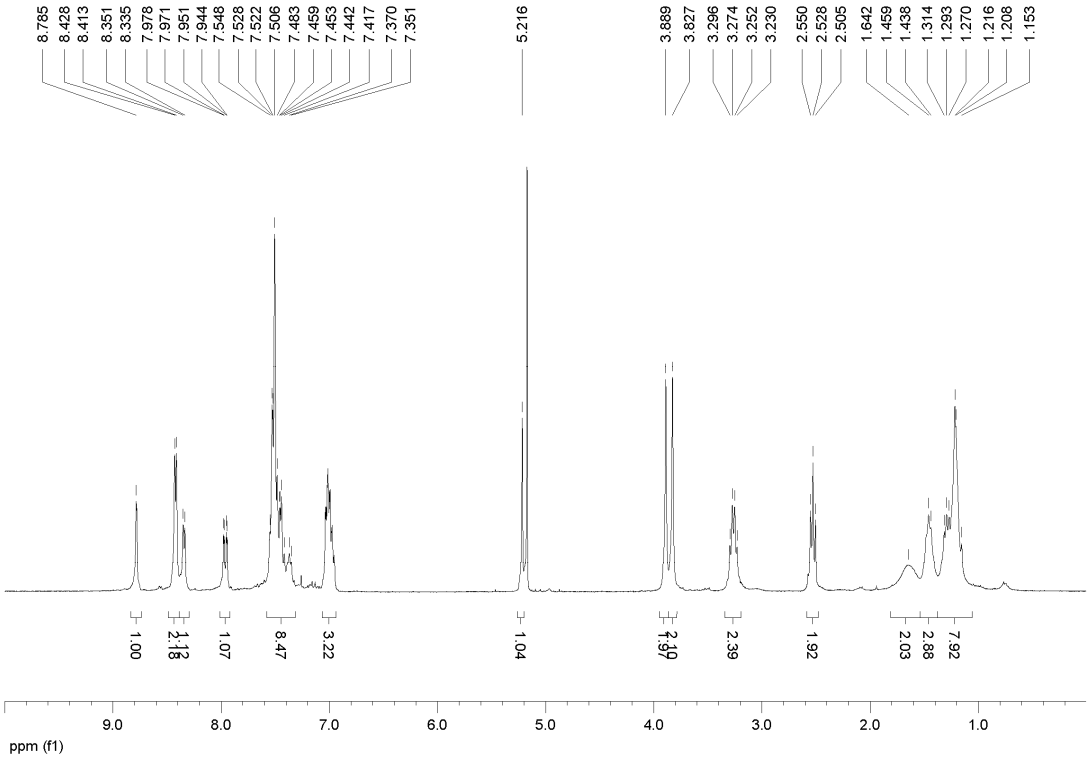

^{13}C NMR spectrum of **3b** ($CDCl_3$, 25 ºC)

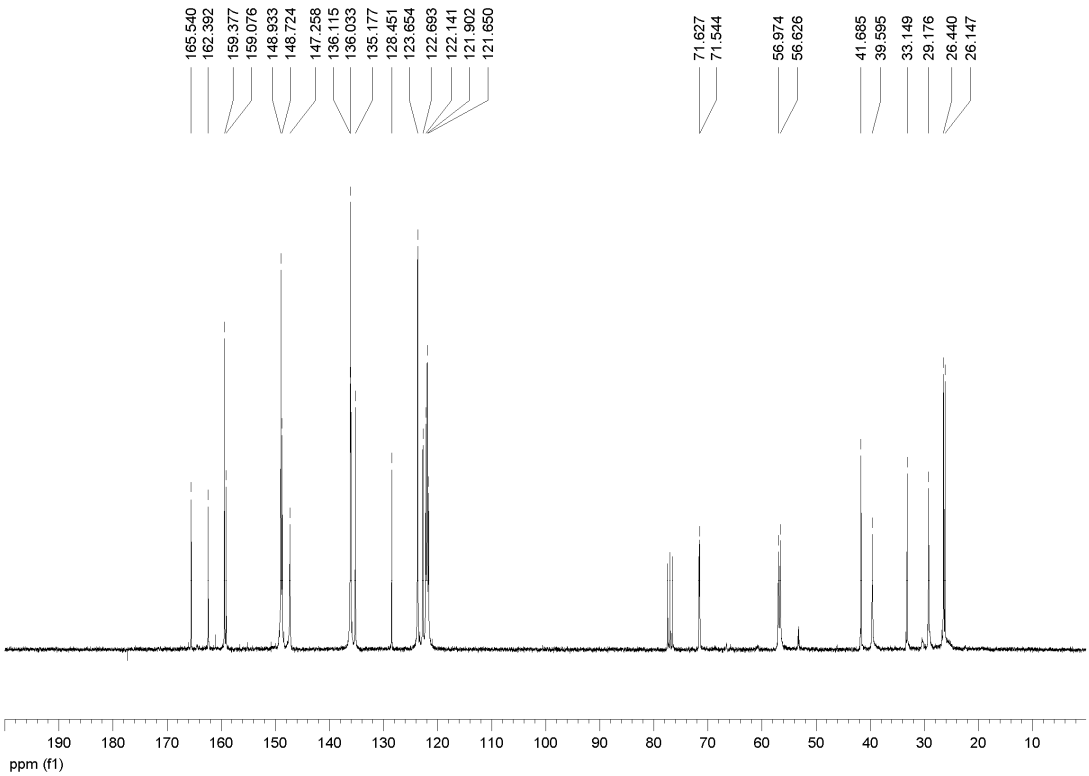

^{1}H NMR spectrum of **3c** (CD_3OD, 25 ºC)

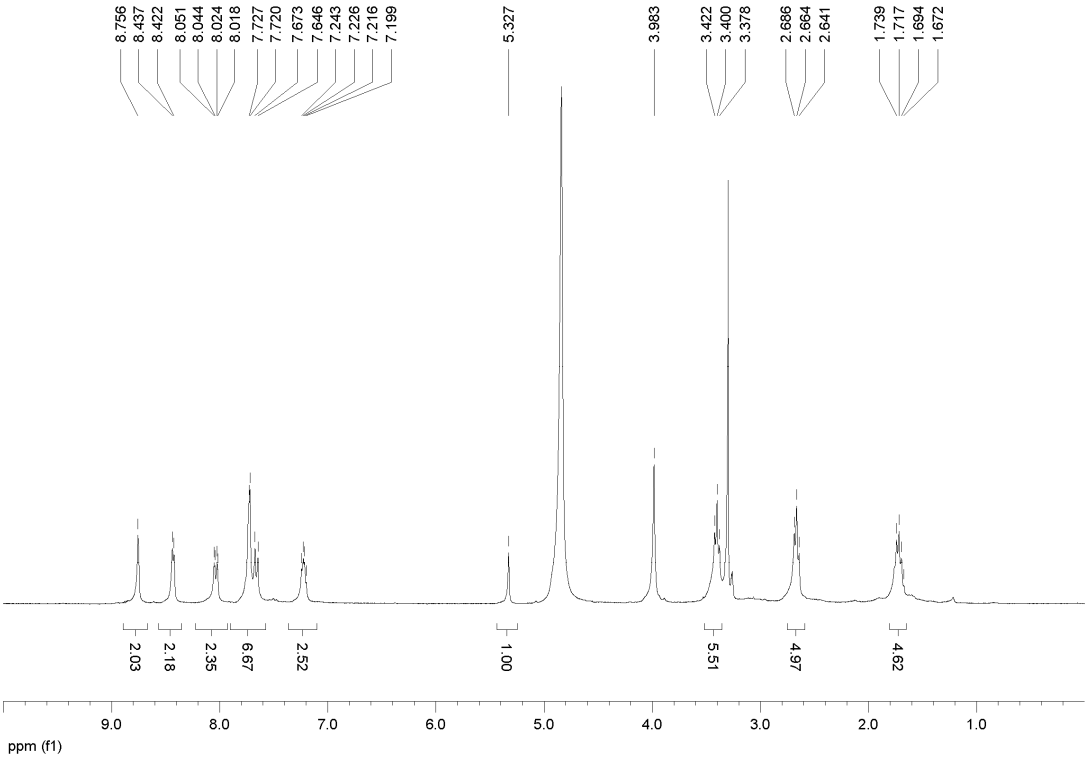

^{13}C NMR spectrum of **3c** (CD_3OD, 25 ºC)

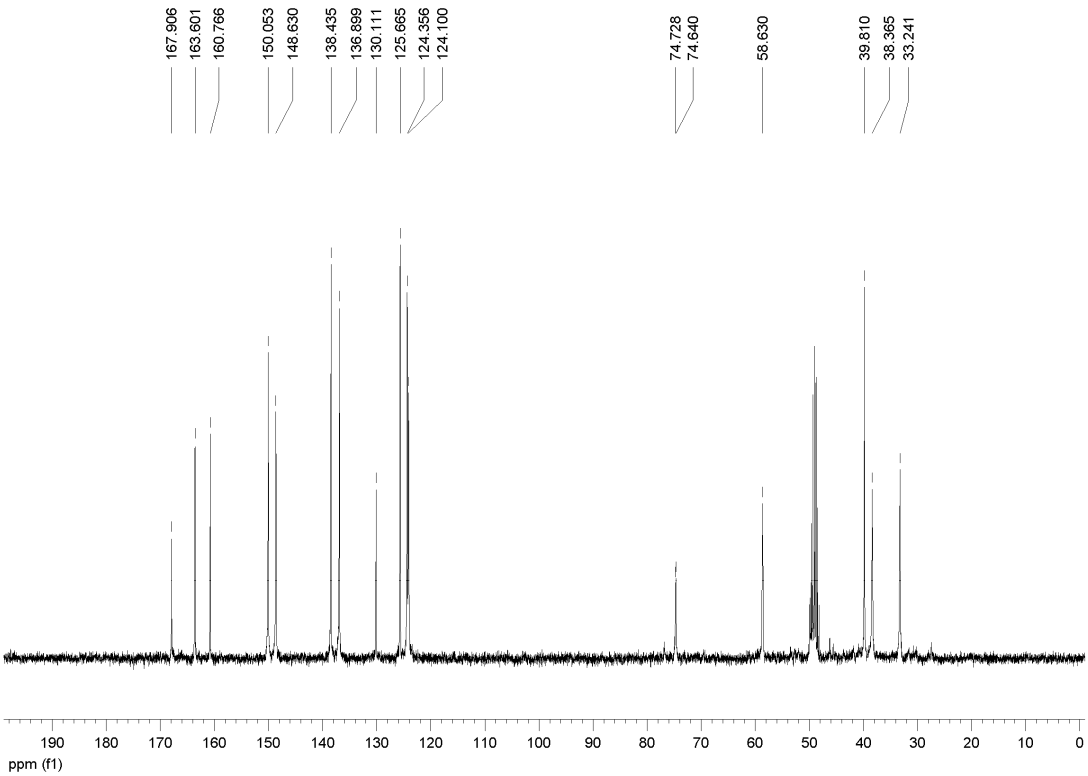

^{1}H NMR spectrum of **4a** ($CDCl_3$, 25 ºC)

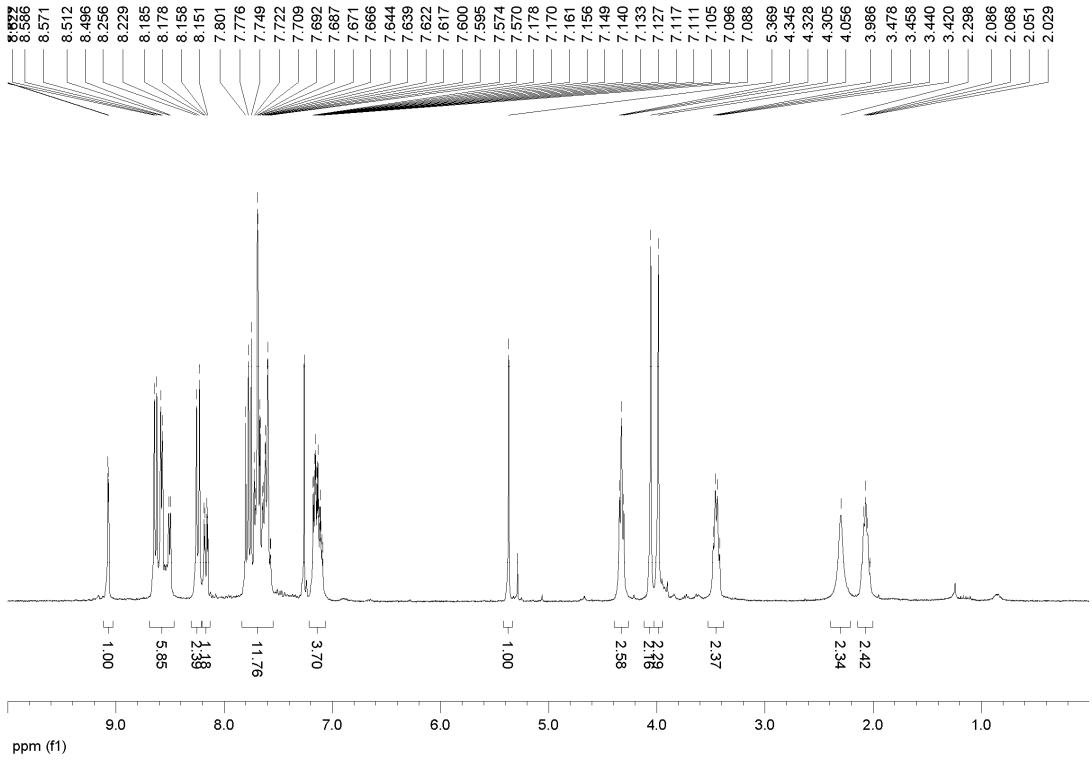

^{13}C NMR spectrum of **4a** ($CDCl_3$, 25 ºC)

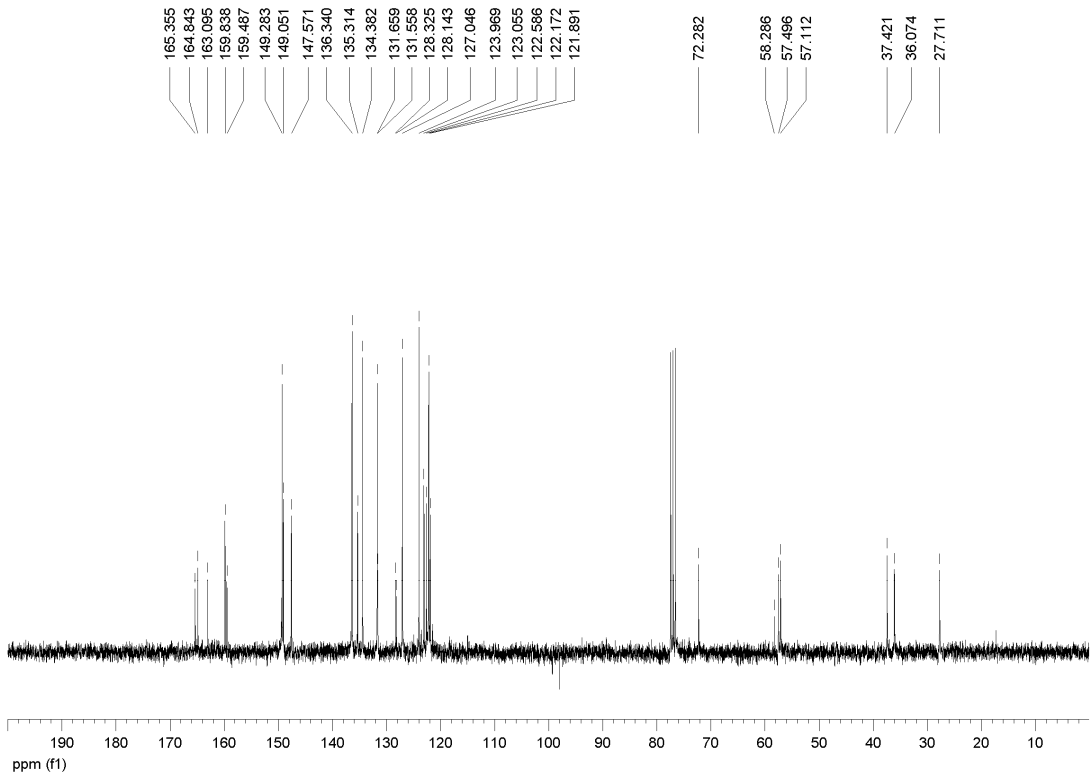

^{1}H NMR spectrum of **4b** ($CDCl_3$, 25 ºC)

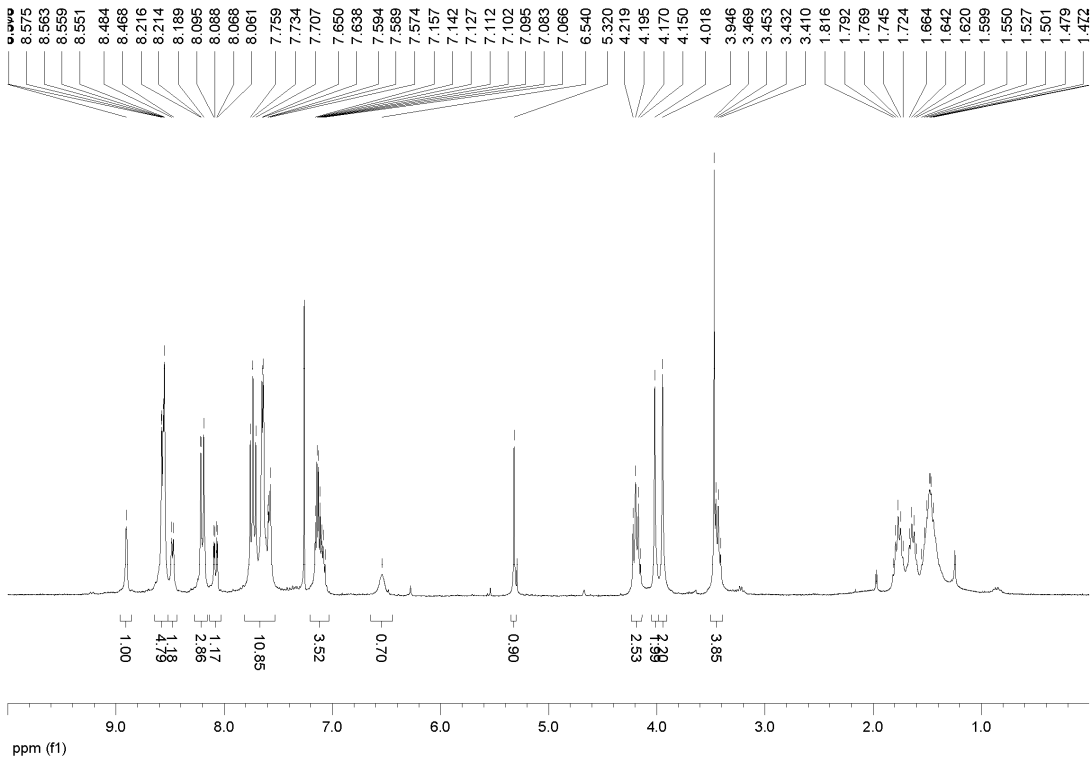

^{13}C NMR spectrum of **4b** ($CDCl_3$, 25 ºC)

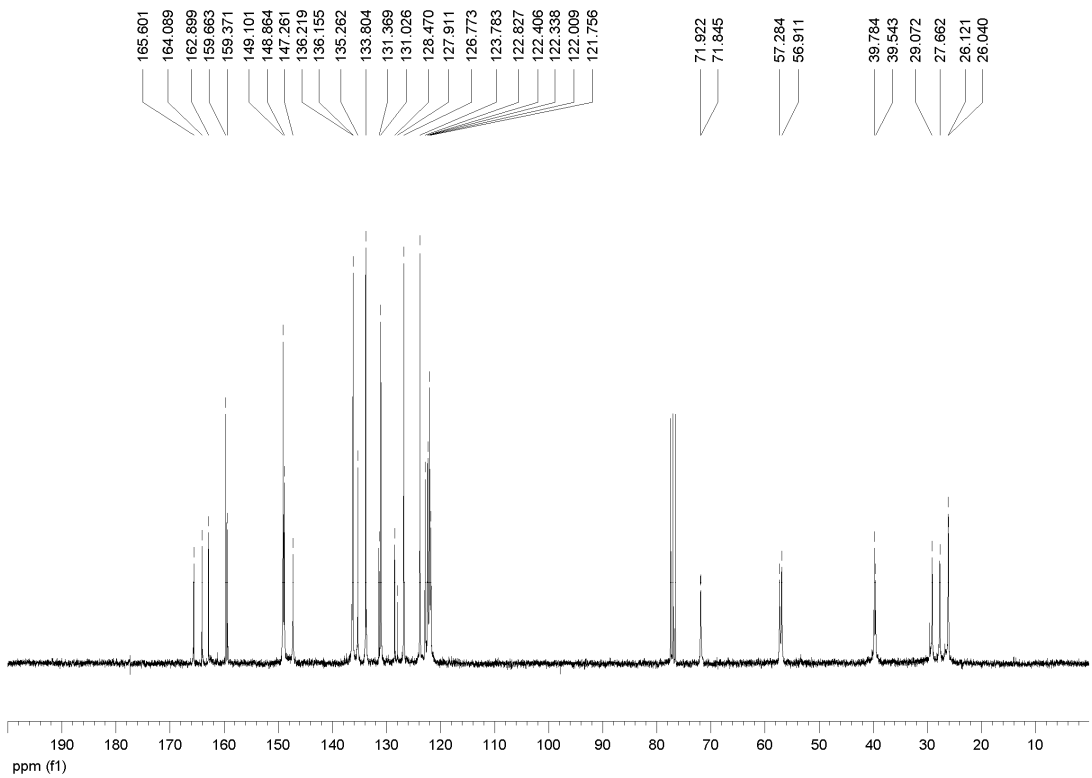

^{1}H NMR spectrum of **4c** ($CDCl_3$, 25 ºC)

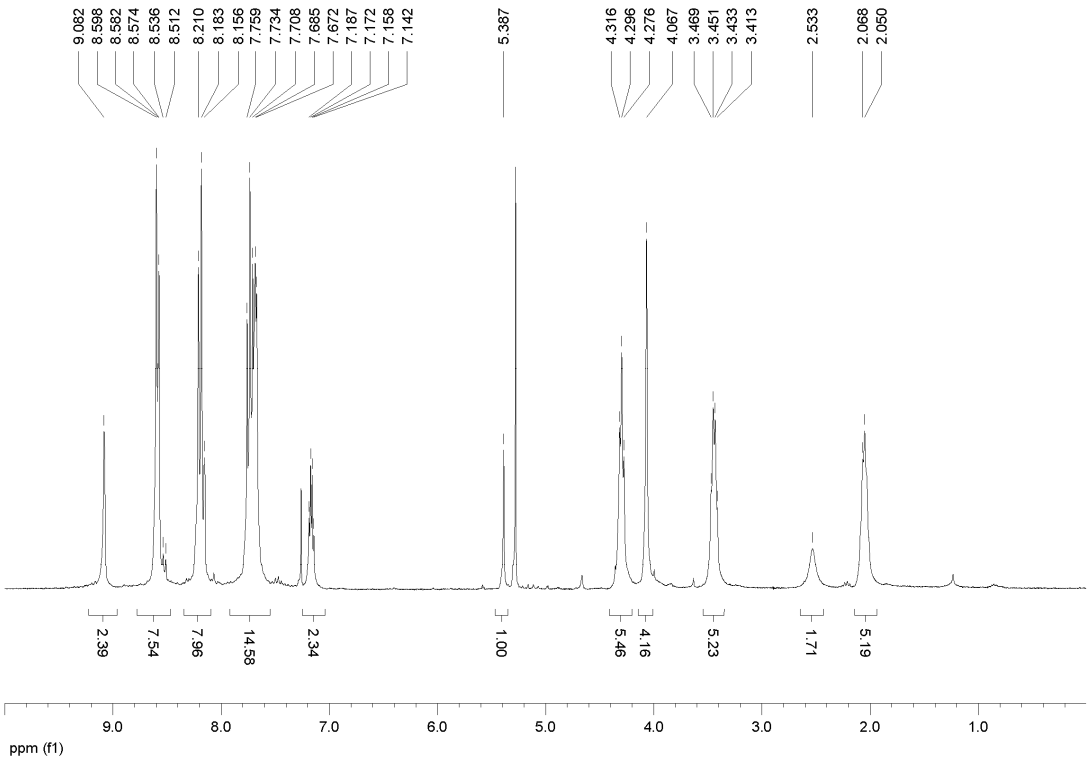

^{13}C NMR spectrum of **4c** ($CDCl_3$, 25 ºC)